

5-10-2019

Are H_0 and σ_8 Tensions Generic to Present Cosmological Data?

Archita Bhattacharyya
Indian Statistical Institute, Kolkata

Ujjaini Alam
Indian Statistical Institute, Kolkata

Kanhaiya Lal Pandey
Indian Institute of Astrophysics

Subinoy Das
Indian Institute of Astrophysics

Supratik Pal
Indian Statistical Institute, Kolkata

Follow this and additional works at: <https://digitalcommons.isical.ac.in/journal-articles>


Recommended Citation

Bhattacharyya, Archita; Alam, Ujjaini; Pandey, Kanhaiya Lal; Das, Subinoy; and Pal, Supratik, "Are H_0 and σ_8 Tensions Generic to Present Cosmological Data?" (2019). *Journal Articles*. 841.
<https://digitalcommons.isical.ac.in/journal-articles/841>

This Research Article is brought to you for free and open access by the Scholarly Publications at ISI Digital Commons. It has been accepted for inclusion in Journal Articles by an authorized administrator of ISI Digital Commons. For more information, please contact ksatpathy@gmail.com.



Are H_0 and σ_8 Tensions Generic to Present Cosmological Data?

Archita Bhattacharyya¹, Ujjaini Alam^{1,2}, Kanhaiya Lal Pandey³ , Subinoy Das³, and Supratik Pal¹¹Physics & Applied Mathematics Unit, Indian Statistical Institute, Kolkata, India; ujjaini.alam@gmail.com²IRAP, Université de Toulouse, CNRS, UPS, CNES, Toulouse, France³Indian Institute of Astrophysics, Bangalore, India

Received 2018 May 28; revised 2019 January 25; accepted 2019 March 23; published 2019 May 14

Abstract

Yes, for a wide range of cosmological models (Λ CDM, non-interacting w_z CDM, w_z WDM, or a class of interacting DMDE). Recently there have been attempts to solve the tension between direct measurements of H_0 and $\sigma_8\sqrt{\Omega_{0m}}$ from respective low-redshift observables and indirect measurements of these quantities from observations of the cosmic microwave background (CMB). In this work we construct a quasi-model-independent framework that reduces to different classes of cosmological models under suitable choices of parameters. We test this parameterization against the latest *Planck* CMB data combined with recent measurements of baryon acoustic oscillations (BAO) and supernovae, and direct measurements of H_0 . Our analysis reveals that a strong positive correlation between H_0 and σ_8 is more or less generic for most of the cosmological models. The present data slightly prefer a phantom equation of state for dark energy and a slightly negative effective equation of state for dark matter (a direct signature of interacting models), with a relatively high H_0 consistent with *Planck*+R16 data and simultaneously a consistent Ω_{0m} . Thus, even though the tensions cannot be fully resolved, a class of interacting models with phantom w_{DE} get a slight edge over w_z CDM for the present data. However, although they may resolve the tension between high-redshift CMB data and individual low-redshift data sets, these data sets have inconsistencies between them (e.g., between BAO and H_0 , supernovae and BAO, and cluster counts and H_0).

Key words: cosmological parameters – dark energy – dark matter

1. Introduction

In the current data-driven era of cosmology, one of the major challenges is to illuminate the dark sector of the universe. Since visible matter has been found to constitute a tiny fraction of the total matter content of the universe, we need to comprehend the nature of dark matter, which comprises nearly a third of the total energy content. Dark energy, the enigmatic negative pressure component that dominates the universe today and causes its expansion to accelerate, is an even greater mystery. The standard cosmological model for the universe is the Λ CDM model, where dark matter is expected to be “cold,” with an equation of state $w_{DM} = 0$, while dark energy is represented by the cosmological constant, with a constant energy density and constant equation of state $w_{DE} = -1$. Current observations are more or less commensurate with this “concordance” model (Ade et al. 2016), with one or two caveats. However, other models for dark matter and dark energy are yet to be ruled out. For dark energy especially, constraints on its equation of state are broad enough that many different models can be accommodated (see reviews by Sahni & Starobinsky 2000; Padmanabhan 2003; Peebles & Ratra 2003; Sahni 2004; Copeland et al. 2006; Frieman et al. 2008; Durrer & Maartens 2010; Tsujikawa 2010; Nojiri & Odintsov 2011; Clifton et al. 2012; Mortonson et al. 2014; Bahamonde et al. 2018). Dynamical dark energy models can be divided into two broad categories. First, one may consider dark energy as a separate energy component, either a fluid or a scalar field or multiple scalar fields. In the second approach, the acceleration of the universe can be explained by introducing new physics in the gravity sector and modifying Einsteinian gravity. Both types of model have been studied extensively against observations (Alam 2010; Holsclaw et al. 2010; Lazkoz et al. 2012; Zhao et al. 2012; Shafieloo et al. 2013; Busti & Clarkson 2016; Aghamousa et al. 2017; Di Valentino et al.

2017; Moresco & Marulli 2017; Zhai et al. 2017; Yu et al. 2018; Gómez-Valent & Amendola 2018), and although recent observations of gravity waves have placed tight constraints on a large number of modified gravity models, many other dark energy models still remain viable. Coupled or interacting dark matter–dark energy (DMDE) models are also in vogue. Though observations suggest that the dark sectors are mostly non-interacting, mild interaction between them cannot be ruled out. In these models, a coupling in the dark sector allows for either dark matter particles to transfer energy into dark energy, or conversely, for dark energy to decay into dark matter on the Hubble timescale. Many different phenomenological forms have been proposed for the interaction and tested against data (Amendola 1999, 2004; Billyard & Coley 2000; Holden & Wands 2000; Hwang & Noh 2002; Chimento et al. 2003; Comelli et al. 2003; Farrar & Peebles 2004; Das et al. 2006; Bean et al. 2008; Lopez Honorez et al. 2010; Beyer et al. 2011; Pavan et al. 2012; Pettorino et al. 2012; Tarrant et al. 2012; Poursidou et al. 2013; Valiviita & Palmgren 2015; Di Valentino et al. 2017; Kumar & Nunes 2017; Mishra & Sahni 2018), but it is difficult to discriminate between the different interacting DMDE models. Also, for these phenomenological models, the results crucially depend on the somewhat ad hoc choice of the interaction term.

The different models for cosmology, be it Λ CDM, or models that fall under the class of either non-interacting w_z CDM or interacting DMDE, or warm dark matter models, are usually constrained against a plethora of observations, including those of the cosmic microwave background (CMB), baryonic acoustic oscillations (BAO), Type Ia supernovae (SNe Ia), measurements of the Hubble parameter $H(z)$ from galaxies, direct measurements of the Hubble constant H_0 , and weak and strong lensing.

It is noteworthy that there appear to be some inconsistencies between different cosmological data sets when analyzed against the concordance Λ CDM model. For example, a major discrepancy between observations arises in the measured value of the Hubble parameter at present. The *Planck* 2015 CMB analysis for the Λ CDM three-neutrino model gives a value of $H_0 = 67.3 \pm 1.0 \text{ km s}^{-1} \text{ Mpc}^{-1}$ (Ade et al. 2016). However, the most recent data set for direct measurement of H_0 (Riess et al. 2016) obtains a 2.4% determination of the Hubble constant at $H_0 = 73.24 \pm 1.74 \text{ km s}^{-1} \text{ Mpc}^{-1}$. This value disagrees at around $\sim 3\sigma$ with that predicted by *Planck*. This is probably the most persistent tension between cosmological data sets for Λ CDM. Another major source of tension is in the predicted values of Ω_{0m} and σ_8 from the CMB and from clusters. From *Planck*, we obtain the constraints $\sigma_8 \sqrt{\Omega_{0m}/0.3} = 0.851 \pm 0.013$, while the clusters provide a lower value of $\sigma_8 \sqrt{\Omega_{0m}/0.3} = 0.745 \pm 0.039$ (Bohringer et al. 2014), a tension at about 2.5σ . Further, recent BAO measurements in the Ly α forest of BOSS DR11 quasars at redshift $z = 2.34$ (Delubac et al. 2014) provide a Hubble parameter of $H(z = 2.34) = 222 \pm 5 \text{ km s}^{-1} \text{ Mpc}^{-1}$, which is 7% higher than the predictions of a flat Λ CDM cosmological model with the best-fit *Planck* parameters, a discrepancy significant at 2.5σ . In yet another departure, the lensing parameter A_L is expected to have the base value of unity for Λ CDM, but has instead constraints of $A_L = 1.22 \pm 0.1$ from *Planck* (Ade et al. 2016). Explanations for these tensions may be found in the errors and systematics in the observations themselves, e.g., different methods of analysis used for the low-redshift SNe Ia data (Efstathiou 2014; Alam & Lasue 2017), possible systematic bias in scaling relations for clusters (Mantz et al. 2015), tensions of the Ly α BAO data with lower-redshift galaxy BAO data (Aubourg et al. 2015; Alam et al. 2017), etc. However, since these tensions seem to exist largely between the high-redshift CMB data and low-redshift direct measurements, this might also be interpreted as a hint to go beyond the standard Λ CDM model and look for new physics that changes the expansion history either at high redshift (by changing N_{eff} , the radiation content (Karwal & Kamionkowski 2016)) or at low redshift (by changing the dark energy dynamics). In this work we explore whether a richer dark sector can provide us an alternative explanation for these discrepancies.

In order to investigate the above-mentioned issues, we analytically reconstruct a model-independent approach to address different classes of cosmological models. We start with the most general interacting DMDE scenario that takes into account the maximum number of model parameters, and construct a framework to deal with the background and perturbation equations in terms of a set of model parameters (namely, the equations of state and sound speed for DM and DE). We also demonstrate that the concordance Λ CDM and non-interacting w_z CDM models turn out to be special cases of this generalized scenario, with a suitable choice of model parameters. Thus, we end up with a framework that takes into account a wide class of cosmological models, thereby making our subsequent investigation of the H_0 and σ_8 discrepancies generic and quasi-model-independent. Then we analyze the current observations against our quasi-model-independent reconstruction of cosmological models followed by a comparison among different cosmological models (Λ CDM, non-interacting w_z CDM, interacting DMDE, warm dark matter

models) and examining the role of each data set in these classes of models.

The plan of the paper is as follows: in Section 2, we outline the quasi-model-independent scheme used to represent different cosmological models, Section 3 describes the data and methodology used in the analysis, Section 4 gives the results, comparison among different models, and discussions, and in Section 5 we present our conclusions.

2. General Framework for Different Cosmological Models

We start with a general theoretical framework where there are two fluids, namely dark energy and dark matter, which may or may not be interacting with each other, and express a set of working formulae, namely the background and perturbation equations, in a general approach. As we shall show subsequently, the usual Λ CDM, the non-interacting w_z CDM, a class of interacting dark sector models as well as warm dark matter models can be considered subsets of this generic framework with a suitable choice of parameters, thereby making the analysis a fairly comprehensive framework for a wide class of different cosmological models.

In this generic setup of (non)interacting dark sectors, different models of the universe have been suggested in the literature and tested against data with varying degrees of success. There is no clear theoretical preference for one model over the others, the various models naturally come up with different constraints on the parameter space, and are therefore difficult to compare. In this work, we aim to recast the evolution equations in a way that allows us to include a wide class of cosmological models, namely Λ CDM, non-interacting w_z CDM, a class of interacting dark sector models, as well as warm dark matter models, by suitably choosing the corresponding parameters.

2.1. Background Equations

The general evolution equations for a two-fluid (DM, DE) interacting cosmological system are obtained from conservation of total energy density to be

$$\rho'_{\text{DM}} + 3\mathcal{H}(1 + w_{\text{DM}})\rho_{\text{DM}} = -aQ \quad (1)$$

$$\rho'_{\text{DE}} + 3\mathcal{H}(1 + w_{\text{DE}})\rho_{\text{DE}} = aQ, \quad (2)$$

where derivatives are taken with respect to the conformal time, and Q is the rate of transfer of energy density, i.e., the interaction term. When the interaction term is switched off ($Q = 0$), we regain the non-interacting DM+DE scenario, while a non-zero Q implies interaction between DM and DE. Usually, when studying interacting DMDE models, Q is replaced by some functional form, e.g., $Q = -\Gamma\rho_{\text{DM}}$ (Boehmer et al. 2008) or $Q = \mathcal{H}(\alpha_{\text{DM}}\rho_{\text{DM}} + \alpha_{\text{DE}}\rho_{\text{DE}})$ (Zimdahl & Pavon 2001). Many different interaction terms have been suggested, some motivated physically, others simple phenomenological parameterizations. On the other hand, $w_{\text{DM}} = 0$ reduces to standard CDM, while a small non-zero w_{DM} would give us warm dark matter, which may or may not interact with dark energy depending on the value of Q . As we will show subsequently, even though the above two equations represent interacting dark sectors, they have the potential to take into account a wide class of cosmological models under consideration.

In order to encompass both the possibilities of warm dark matter and interacting DMDE with fewer parameters, as well as to take into account the usual Λ CDM and non-interacting w_z CDM, we recast the above equations to resemble the non-interacting w_z CDM scenario (Valiviita et al. 2008):

$$\rho'_{\text{DM,eff}} + 3\mathcal{H}(1 + w_{\text{DM,eff}})\rho_{\text{DM,eff}} = 0 \quad (3)$$

$$\rho'_{\text{DE,eff}} + 3\mathcal{H}(1 + w_{\text{DE,eff}})\rho_{\text{DE,eff}} = 0, \quad (4)$$

with the effective equations of state for dark matter and dark energy defined by adding the effect of the interaction term Q to the true dark matter and dark energy equations of state:

$$w_{\text{DM,eff}} = w_{\text{DM}} + \frac{aQ}{3\mathcal{H}\rho_{\text{DM}}} \quad (5)$$

$$w_{\text{DE,eff}} = w_{\text{DE}} - \frac{aQ}{3\mathcal{H}\rho_{\text{DE}}}. \quad (6)$$

In the interacting scenario, for $Q > 0$, energy is transferred from dark matter to dark energy, which implies $w_{\text{DM,eff}} > 0$; the effective dark matter redshifts at a rate faster than a^{-3} , and $w_{\text{DE,eff}} < w_{\text{DE}}$; the effective dark energy has more negative pressure. For $Q < 0$, the opposite happens. In the non-interacting scenario, $w_{\text{DM,eff}} \neq 0$ implies non-cold dark matter.

We note here that, for a constant $w_{\text{DM,eff}} - w_{\text{DM}}$, this approach takes care of a class of interacting dark sector models where $Q \propto \mathcal{H}\rho_{\text{DM}}$. Apart from this class of interacting models, this approach also has the added advantage that it boils down to different classes of dark sector models by suitable choices of its parameters, namely $w_{\text{DM,eff}}$ and $w_{\text{DE,eff}}$:

1. $w_{\text{DM,eff}} = 0$, $w_{\text{DE,eff}} = -1$ (Λ CDM),
2. $w_{\text{DM,eff}} = 0$, $w_{\text{DE,eff}} < -1$ (phantom), > -1 (non-phantom), (non-interacting w_z CDM, depending on scalar field or modified gravity models),
3. $w_{\text{DM,eff}} \neq 0$ (warm dark matter models or a class of interacting dark sector models).

Strictly speaking, although $w_{\text{DM,eff}}$ and $w_{\text{DE,eff}}$ are independent parameters for all other cosmological models (Λ CDM, non-interacting w_z CDM, modified gravity, and warm dark matter models), they are not strictly independent free parameters for the interacting DMDE models under consideration, because of the coupling term Q . However, one cannot have any a priori knowledge of the interaction term from theoretical perspectives alone, even if there is any such interaction between dark matter and dark energy. In order to have an idea of the interaction, one needs observational data. As will be revealed in due course, observational data put stringent constraints on any possible interaction, and DMDE interaction, if any, would be really feeble, deviating from $w_{\text{DM,eff}} = 0$ by a very tiny amount at the most, so that we could *effectively* decouple the equations of state. As a result, this parameterization allows us to consider them as independent parameters for all practical purposes. This is what we are going to consider in the present article.

2.2. Linear Perturbations

In this approach, the perturbation equations need to be similarly recast in terms of effective equations of state for dark matter and dark energy, so that the interaction term Q does not explicitly appear in them (or, in turn, the effects of warm dark

matter, if any, become obvious). Scalar perturbations on a flat FRW metric are given by

$$ds^2 = a^2 \{ -(1 + 2\psi)d\eta^2 + 2\partial_i B d\eta dx^i + [(1 - 2\phi)\delta_{ij} + 2\partial_i \partial_j E] dx^i dx^j \}. \quad (7)$$

The energy–momentum tensor for the dark sector is given by

$$T_\nu^\mu = (\rho + P)u^\mu u_\nu + P\delta_\nu^\mu, \quad (8)$$

where $\rho = \bar{\rho} + \delta\rho$, $P = \bar{P} + \delta P$, the background 4-velocity is $\bar{u}^\mu = a^{-1}\delta_0^\mu$ and the perturbed 4-velocity is given by $u^\mu = a^{-1}(1 - \psi, \partial^i v)$, $u_\mu = a(-1 - \psi, \partial_i[v + B])$, with v as the peculiar velocity potential. We adopt the synchronous gauge for which $\psi = B = 0$, $\phi = \eta$, and $k^2 E = -h/2 - 3\eta$.

For a coupled (or an uncoupled) dark sector scenario, the pressure perturbation for each component is

$$\delta P_i = c_{ai}^2 \delta\rho_i + (c_{si}^2 - c_{ai}^2)[3\mathcal{H}(1 + w_{i,\text{eff}})\rho_i] \frac{\theta_i}{k^2}, \quad (9)$$

where $i = \text{DM, DE}$. Therefore the background coupling enters δP_i through the term $w_{i,\text{eff}}$. The effective sound speed $c_{si,\text{eff}}$ of a fluid in its rest frame is then defined as

$$c_{si,\text{eff}}^2 = \frac{\delta P_i}{\delta\rho_i}, \quad (10)$$

and the adiabatic sound speed as

$$c_{ai,\text{eff}}^2 = \frac{P_i'}{\rho_i'} = w_{i,\text{eff}} + \frac{w_{i,\text{eff}}'}{\rho_i'/\rho_i}. \quad (11)$$

It is worth pointing out here that that the effective sound speeds reduce to the standard sound speeds of non-interacting w_z CDM and Λ CDM as soon as the interaction term is switched off.

Using the above definitions, we may now write down the effective perturbed evolution equations for DM and DE as

$$\begin{aligned} \delta'_{\text{DM}} + 3\mathcal{H}(c_{\text{sDM,eff}}^2 - w_{\text{DM,eff}})\delta_{\text{DM}} + (1 + w_{\text{DM,eff}})\theta_{\text{DM}} \\ + 9\mathcal{H}^2[(1 + w_{\text{DM,eff}})(c_{\text{sDM,eff}}^2 - w_{\text{DM,eff}})] \frac{\theta_{\text{DM}}}{k^2} \\ = (1 + w_{\text{DM,eff}}) \frac{h'}{2} \end{aligned} \quad (12)$$

$$\theta'_{\text{DM}} + (1 - 3c_{\text{sDM,eff}}^2)\theta_{\text{DM}} - \frac{c_{\text{sDM,eff}}^2}{1 + w_{\text{DM,eff}}} k^2 \delta_{\text{DM}} = 0 \quad (13)$$

$$\begin{aligned} \delta'_{\text{DE}} + 3\mathcal{H}(c_{\text{sDE,eff}}^2 - w_{\text{DE,eff}})\delta_{\text{DE}} + (1 + w_{\text{DE,eff}})\theta_{\text{DE}} \\ + 9\mathcal{H}^2 \left[(1 + w_{\text{DE,eff}})(c_{\text{sDE,eff}}^2 - w_{\text{DE,eff}}) + \frac{w'_{\text{DE,eff}}}{3\mathcal{H}} \right] \frac{\theta_{\text{DE}}}{k^2} \\ = (1 + w_{\text{DE,eff}}) \frac{h'}{2} \end{aligned} \quad (14)$$

$$\theta'_{\text{DE}} + (1 - 3c_{\text{sDE,eff}}^2)\theta_{\text{DE}} - \frac{c_{\text{sDE,eff}}^2}{1 + w_{\text{DE,eff}}} k^2 \delta_{\text{DE}} = 0. \quad (15)$$

We note here that, in the synchronous gauge, DM particles are typically taken as gauge coordinates so that θ_{DM} vanishes. But in our setup we need to consider the equation for θ_{DM} as well since there is non-zero momentum transfer in the DM frame. We have checked that in the limits

$w_{\text{DM,eff}} = 0$, $w_{\text{DM,eff}} = -1$, $c_{\text{sDM,eff}}^2 = 0$, $c_{\text{sDE,eff}}^2 = 1$, i.e., in the non-interacting scenario, this framing of equations provides the same result as in the standard synchronous gauge setup.

It is now straightforward to verify that the above set of perturbation equations represent a broad class of cosmological models under consideration. They readily boil down to the six-parameter Λ CDM and non-interacting w_z CDM, modified gravity or warm dark matter models with the following choice of parameters:

1. $w_{\text{DM,eff}} = 0$, $w_{\text{DE,eff}} = -1$, $c_{\text{sDM,eff}}^2 = 0$, $c_{\text{sDE,eff}}^2 = 1$ (Λ CDM).
2. $w_{\text{DM,eff}} = 0$, $w_{\text{DE,eff}} < -1$ (phantom) or > -1 (non-phantom), $c_{\text{sDM,eff}}^2 = 0$, $c_{\text{sDE,eff}}^2 = 1$ or $\neq 1$ (depending on non-interacting w_z CDM or modified gravity models).
3. $w_{\text{DM,eff}} \neq 0$, $w_{\text{DE,eff}} = -1$, $c_{\text{sDM,eff}}^2 = 0$, $c_{\text{sDE,eff}}^2 = 1$ (Λ WDM).
4. $w_{\text{DM,eff}} \neq 0$, $w_{\text{DE,eff}} < -1$ or > -1 , $c_{\text{sDM,eff}}^2 = 0$ or $\neq 0$, $c_{\text{sDE,eff}}^2 = 1$ or $\neq 1$ (for more complicated warm dark matter models, such as w_z WDM).

Thus, in a nutshell, we have in our hand a set of background and perturbation equations for a wide class of cosmological models in terms of the *effective* equations of state and *effective* sound speeds. Constraining these effective parameters from data in turn results in studying the pros and cons of different class of cosmological models in this framework. As already stated, in the rest of the article we are going to primarily address two major tensions of modern cosmology, namely the values of H_0 and σ_8 from different low- and high-redshift data, using the framework described above.

3. Methodology

We may now test our model-independent framework against currently available data. Many different cosmological observations are sensitive to the dark sector. To constrain different class of cosmological models, both background expansion data and perturbative data may be utilized. The primary goal in this work is to investigate whether the inconsistencies in the low- and high-redshift data can be resolved in *any* class of the cosmological models using this model-independent framework. We concentrate on the following data sets:

1. CMB: *Planck* TT and low- l data from the *Planck* 2015 data release (Ade et al. 2016).
2. Galaxy BAO: Measurements from 6dFGS at $z = 0.106$ and MGS at $z = 0.15$ from the Sloan Digital Sky Survey (SDSS), as well as the CMASS and LOW z samples from BOSS DR12 at $z = 0.38, 0.51, \text{ and } 0.61$ (Alam et al. 2017).
3. SNe Ia: SNe Ia data from the Joint Light-curve Analysis (JLA) of SDSS-II and SNLS3 (Betoule et al. 2014).
4. H_0 : Recent direct measurement of the Hubble constant (Riess et al. 2016), which provides a value of $H_0 = 73.24 \pm 1.74 \text{ km s}^{-1} \text{ Mpc}^{-1}$.

The combination of data sets outlined above is neither exhaustive nor complete, and other works are available that provide somewhat different takes on some of these data sets. For example, direct measurements of H_0 are subject to various tensions. The early *HST* Cepheid+SNe based estimate from Riess et al. (2011) gives $H_0 = 73.8 \pm 2.4 \text{ km s}^{-1} \text{ Mpc}^{-1}$. The same Cepheid data have been analyzed by Efstathiou (2014)

using a revised geometric maser distance to NGC 4258. Using NGC 4258 as a distance anchor, he finds $H_0 = 70.6 \pm 3.3 \text{ km s}^{-1} \text{ Mpc}^{-1}$. The more recent paper (Riess et al. 2016) obtains a 2.4% determination of the Hubble constant at $H_0 = 73.24 \pm 1.74 \text{ km s}^{-1} \text{ Mpc}^{-1}$ by combining the anchor NGC 4258, the Milky Way, and LMC Cepheids. The Milky Way Cepheid solutions for H_0 may be unstable (Efstathiou 2014), which could go some way in explaining this inconsistency. However, recent observations of strong lensing (Bonvin et al. 2017) also give the slightly higher value of $H_0 = 71.9_{-3.0}^{+2.4} \text{ km s}^{-1} \text{ Mpc}^{-1}$. On the other hand, measurements of the Hubble parameter from SNe and red giant halo populations (Tammann & Reindl 2013) give $H_0 = 63.7 \pm 2.3 \text{ km s}^{-1} \text{ Mpc}^{-1}$. A recent measurement of the Hubble parameter by Chen et al. (2017) prefers a value of $H_0 = 68.3_{-2.6}^{+2.7} \text{ km s}^{-1} \text{ Mpc}^{-1}$, which is more in line with the *Planck* results. The most recent SDSS DR12 BAO data (Alam et al. 2017) also appear to favor a somewhat lower value of $H_0 = 67.8 \pm 1.2 \text{ km s}^{-1} \text{ Mpc}^{-1}$. Thus as yet there is no clear consensus about the value of H_0 . We have chosen to use the result from Riess et al. (2016, hereafter R16) since this is the latest direct measurement of H_0 , and it is clearly in tension with CMB.

Similarly, although cluster counts for X-ray-selected clusters from REFLEX-II provide a lower value of $\sigma_8 \sqrt{\Omega_{\text{m}}/0.3} = 0.745 \pm 0.039$ (Bohringer et al. 2014) than *Planck*, an analysis of cluster counts of X-ray-selected clusters by the WtG collaboration, incorporating the WtG weak lensing mass calibration, finds $\sigma_8 \sqrt{\Omega_{\text{m}}/0.3} = 0.81 \pm 0.03$ (Mantz et al. 2015), in better agreement with the *Planck* CMB results of $\sigma_8 \sqrt{\Omega_{\text{m}}/0.3} = 0.851 \pm 0.013$. This discrepancy within cluster observations may be due to biases in mass calibration or in the assumed scaling relations for clusters selected by the Sunyaev-Zel'dovich effect as compared to X-ray-selected clusters. As in the case of H_0 , here too we shall compare the σ_8 obtained from our analysis with that from the more exhaustive data set (Bohringer et al. 2014), which is in tension with *Planck*, to see whether interaction in the dark sector may alleviate this tension.

Within the BAO data sets, the Ly α BAO results are in more than 2σ tension with the low-redshift galaxy BAO results, and are plagued by various systematics (Aubourg et al. 2015); also the SDSS DR12 for these data has not yet been released, hence we leave the Ly α data out of our analysis at present, and use the galaxy BAO data only.

To determine the likelihoods for our parameters of interest, we perform a Monte Carlo Markov chain analysis with CosmoMC using a modified version of CAMB. Assuming a flat FRW universe, we vary the following cosmological parameters: the physical baryon and DM densities today ($\Omega_b h^2$ and $\Omega_c h^2$), the angular size of the last scattering surface (θ), the optical depth due to reionization (τ), the amplitude of the primordial power spectrum (A_s), the scalar spectral index (n_s), the effective equation of state (EoS) of DE ($w_{\text{DE,eff}}$, which can be further parameterized by its value today w_0 , and its rate of change over the scale factor w_a), the effective EoS of DM ($w_{\text{DM,eff}}$), the effective sound speed of DE ($c_{\text{sDE,eff}}^2$), and the effective sound speed of DM ($c_{\text{sDM,eff}}^2$).

Therefore, in addition to the standard Λ CDM parameters, we now need to constrain the effective parameters $\{w_{\text{DE,eff}}, w_{\text{DM,eff}}, c_{\text{sDE,eff}}^2, c_{\text{sDM,eff}}^2\}$. For the dark energy EoS, we use the well-known model-independent Chevallier-

Polarski–Linder (CPL) parameterization (Chevallier & Polarski 2001; Linder 2003), which takes into account a wide class of dark energy models (and may represent the effective dark energy for interacting models in our formalism) and is represented by

$$w_{\text{DE,eff}} = w_0 + w_a(1 - a). \quad (16)$$

One may wonder whether the above CPL parameterization, which is usually employed for non-interacting dark energy models, can be used in this generalized scenario. We should clarify that at this point. A parameterization is a tool to constrain a number of models from observations. As is well known, data are not directly sensitive to models, but rather to some parameters that represent the background model(s) via the parameterization. As such, CPL is a considerably good parameterization that can take into account most of the non-interacting dark energy models. Since in our formalism we have made the effective equations of state look non-interacting, it can in principle be applied to represent at least this class of models under consideration, even though that encompasses, intrinsically, interacting DMDE models, among others. Nevertheless, as it will turn out in the subsequent section, present data sets constrain $w_{\text{DM,eff}}$ to pretty close to zero, and hence any interaction as such has to be very tiny. As a result, effectively, the $w_{\text{DE,eff}}$ behaves pretty similarly to the EoS of non-interacting models. Hence a CPL parameterization for the class of models under consideration (non-interacting $w_z\text{CDM}$, modified gravity, warm dark matter models, or ΛCDM) is very much a suitable parameterization. The only assumption made here is that in the case of interacting DMDE models, the interaction has to be really feeble, which is indeed the case so far as observational data are concerned.

Thus the Hubble parameter, representing the expansion history of the universe, may be written as

$$H(a) = H_0[\Omega_{0r}a^{-4} + \Omega_{0m}a^{-3(1+w_{\text{DM,eff}})} + (1 - \Omega_{0r} - \Omega_{0m}) \times a^{-3(1+w_0+w_a)}e^{-3w_a(1-a)}]^{1/2}. \quad (17)$$

In this ansatz, the DE EoS may cross the phantom barrier ($w = -1$) at some point of its evolution. Typically, single scalar field models of dark energy cannot have such a phantom crossing since the velocity component of the perturbation equations would blow up at $w_{\text{DE,eff}} = -1$ (see Equation (15)). It is possible to have such a phantom crossing in models with multiple scalar fields representing dark energy (Fang et al. 2008). For this work, we limit ourselves to the simpler single scalar field or modified gravity scenarios and study phantom and non-phantom behavior separately. We use the priors $w_0 \in [-1, -0.33]$ and $[-3, -1]$ for non-phantom and phantom regimes respectively, and $w_a \in [-2, 2]$, $c_{\text{sDE,eff}}^2 \in [0, 2]$. We do not attempt to vary the sound speed of DM because it is very tightly constrained by the available data, and we keep it fixed to zero, as expected for standard cold dark matter. We note here that the parameters varied here, i.e., w_0 , w_a , $w_{\text{DM,eff}}$, $c_{\text{sDE,eff}}^2$, are all effective parameters for DM and DE, which implicitly contain the interaction, if any, between DM and DE. Data being sensitive only to the effective parameters, the true values of w_{DE} , w_{DM} , c_{sDE}^2 are not directly seen in the observables. The presence and nature of interaction, if any, between DM and DE can be surmised from the

deviation of the above effective values from the standard ΛCDM or w_0 , w_a +CDM parameter values. A non-zero value of $w_{\text{DM,eff}}$, for example, could signal either a departure from CDM (e.g., warm dark matter models) or the presence of interaction between CDM and DE. Since available data strongly constrain the ‘‘coldness’’ of dark matter, we interpret any departure from $w_{\text{DM,eff}} = 0$ as the possibility of interaction within the dark sector.

4. Results, Comparison, and Discussions

4.1. Phantom EoS

As pointed out in the last section, we will deal with phantom and non-phantom cases separately. We first show the results for the phantom (non)interacting DMDE models, i.e., models with $w_{\text{DE,eff}} \leq -1$. The parameters of interest are Ω_{0m} , H_0 , σ_8 , w_0 , w_a , $w_{\text{DM,eff}}$, $c_{\text{sDE,eff}}^2$. We wish to see whether opening up the parameter space helps ease the tension in H_0 as well as that in Ω_{0m} , σ_8 . We will also attempt to understand the effect of different data sets on the individual parameters, and hence on different classes of models. We reiterate that when we say ‘‘models’’ here, we have in mind the usual ΛCDM , non-interacting $w_z\text{CDM}$, modified gravity, warm dark matter models as well as a class of interacting DMDE models that can be represented in this theoretical framework described in Section 2. This will in turn constrain the equations of state of dark matter and dark energy directly from observations for this wide class of theoretical models. First, we find that the results are quite insensitive to $c_{\text{sDE,eff}}^2$; freeing up this parameter has little effect on the constraints on the other parameters, and the parameter itself remains fairly unconstrained. We therefore keep it fixed for primary analysis at the scalar field value of $c_{\text{sDE,eff}}^2 = 1$. Figure 1 shows the likelihoods for the remaining parameters using (i) only *Planck* data, (ii) *Planck* with R16 H_0 measurement, (iii) *Planck* with BAO data, (iv) *Planck* with SNe data, and (v) *Planck* with R16 H_0 + BAO + SNe Type Ia data (BSH).

We see that the *Planck* data alone (black lines) do not have a very strong constraining power on the individual parameters. With CMB alone, H_0 , Ω_{0m} , $w_{\text{DM,eff}}$, w_0 , w_a are all fairly unconstrained. The underlying reason is as follows: since we constrain δ_{DM} or its function, and H_0 , $w_{\text{DM,eff}}$, and Ω_{0m} enter the perturbation equations as $w_{\text{DM,eff}}h$ and $\Omega_{0m}h^2$, therefore, although $w_{\text{DM,eff}}h$ and $\Omega_{0m}h^2$ are constrained quite strongly, H_0 , $w_{\text{DM,eff}}$ and Ω_{0m} are individually unconstrained since one can always increase one parameter and decrease another to achieve the same constraint for the combination. The effective dark energy parameters w_0 and w_a enter indirectly through δ_{DE} and therefore metric perturbations, thus they or any function of them is not strongly constrained by CMB.

With the addition of the H_0 measurements, CMB+R16 tightens up constraints on H_0 and therefore on Ω_{0m} , $w_{\text{DM,eff}}$, and consequently on σ_8 (red lines), but provides no further constraining power for the dark energy parameters. As above, this can be understood because w_0 and $w_{\text{DM,eff}}$ enter expansion history similarly. However, the difference between them appears in perturbations. CMB constrains $\Omega_{0m}h^2$ and $w_{\text{DM,eff}}h$, therefore if H_0 is fixed in a range from R16, Ω_{0m} and $w_{\text{DM,eff}}$ also get confined to a fixed narrow range. The same effect is not seen on w_0 or w_a because these or any functions of them are weakly constrained by CMB.

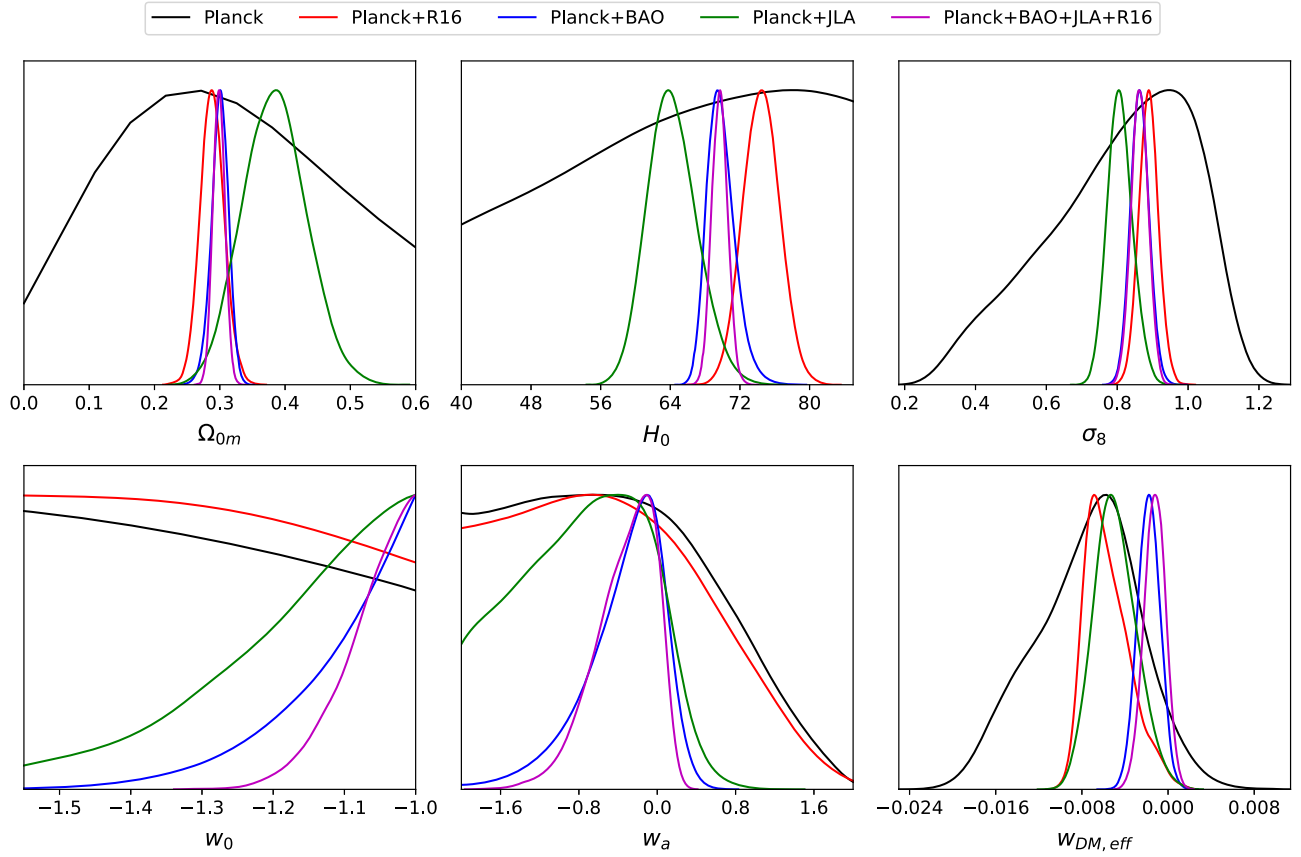


Figure 1. Likelihoods in Ω_{0m} , H_0 , σ_8 , w_0 , w_a , $w_{DM,eff}$ for cosmological reconstruction using *Planck* (black lines), *Planck+R16* (red lines), *Planck+BAO* (blue lines), *Planck+JLA* (green lines), and *Planck+BSH* (magenta lines) for phantom (non)interacting models under consideration.

The addition of BAO to *Planck* data brings the matter density to $\Omega_{0m} \sim 0.3$, which is slightly higher and with narrower errors than the result for *Planck+R16*, but it chooses an H_0 noticeably lower than that favored by *R16*, and also a higher $w_{DM,eff}$ (blue lines). In addition it also provides some constraints on w_0 , w_a . BAO measured either the Hubble parameter or its integral in the form of the angular diameter distance, and from these it tends to put the strongest constraints on Ω_{0m} , and weaker constraints on the other parameters such as H_0 , $w_{DM,eff}$, w_0 , w_a . Adding these new constraints to CMB, we are able to break the degeneracy between Ω_{0m} , H_0 and $w_{DM,eff}$, H_0 . BAO by itself would allow degeneracy between $w_{DM,eff}$ and w_0 , and between $w_{DM,eff}$ and H_0 as well; this degeneracy is broken by constraints from CMB on $w_{DM,eff}h$, $\Omega_{0m}h^2$. Once Ω_{0m} , H_0 , $w_{DM,eff}$ are constrained, the remaining parameters w_0 , w_a get constrained as well. w_a has the weakest constraint since it enters the equation for $H(z)$ to the second order.

Adding the JLA SNe Ia to *Planck* narrows down the constraints like BAO does, but in a different direction. In this case, Ω_{0m} is moved to a higher value than that for either of the two previous cases, and H_0 to a lower value (green lines). $w_{DM,eff}$ is in about the same region as that for *Planck+H_0*. The DE parameters are constrained as well, but less so than in the case for BAO. In this case, we know that JLA+CMB tends to prefer non-phantom DE (Betoule et al. 2014) with $\Omega_{0m} \simeq 0.3$ in the non-interacting case. Here we are adding a new parameter, $w_{DM,eff}$, and constraining the DE parameters to the phantom regime, forcing $w_{DE,eff} \leq -1$. The data may compensate for phantom DE by choosing either (i)

$\Omega_{0m} > 0.3$, $w_{DM,eff} \lesssim 0$ or (ii) $\Omega_{0m} < 0.3$, $w_{DM,eff} \gtrsim 0$. Since the CMB data prefer to keep the new parameter $w_{DM,eff} < 0$, *Planck+JLA* therefore pushes Ω_{0m} to a higher value and consequently H_0 to a lower value. The DE parameters are less constrained than BAO because BAO measures $H(z)$ while SNe data measure the magnitude, which is related to $H(z)$ by an integral and logarithm, thereby reducing its constraining power.

Adding all the data sets together, naturally the constraints are at their narrowest (purple lines); however, given the inconsistencies between the different data sets, the results are not necessarily commensurate with those for the separate data sets. For example, *Planck+R16* obtained a high H_0 , but due to the effect of SNe and BAO, *Planck+BSH* reduces H_0 . Thus though the tension between CMB and direct H_0 is resolved for a slightly negative $w_{DM,eff}$, *Planck+BSH* does not completely agree with the direct H_0 measurements.

Figure 2 shows the 1σ and 2σ confidence levels in the $H_0 - w_{DM,eff}$, $\Omega_{0m} - \sigma_8$, and $w_0 - w_a$ parameter spaces for the three different data sets. We see here that the *Planck* confidence levels in H_0 are very large (gray contours of left panel), mainly due to the flexibility afforded by the new parameter $w_{DM,eff}$. For small negative values of $w_{DM,eff}$, therefore, H_0 from *Planck* data is allowed to go up to much larger values than those allowed by Λ CDM, thereby reducing its tension with the direct measurement of H_0 (as evinced from the red contours in the left panel). The addition of BAO and SNe data, however, slightly disfavors non-zero $w_{DM,eff}$, and the tension in H_0 resumes somewhat.

Further, due to the freeing-up of H_0 , the $\Omega_{0m} - \sigma_8$ parameter space is also opened up, with lower values of σ_8 chosen for

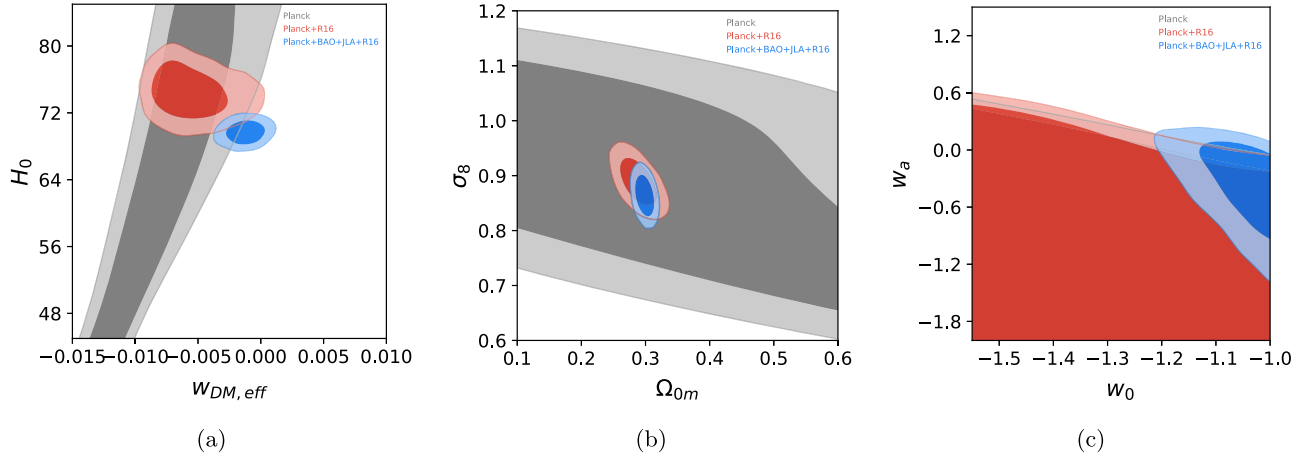


Figure 2. 1σ and 2σ confidence levels in the $H_0 - w_{\text{DM,eff}}$ (left panel), $\Omega_{0m} - \sigma_8$ (middle panel), and $w_0 - w_a$ (right panel) parameter spaces using *Planck* (gray), *Planck+R16* (red), and *Planck+BSH* (blue) for phantom (non)interacting models under consideration.

Table 1

Best-fit and 1σ Values for Ω_{0m} , H_0 , σ_8 , w_0 , w_a , $w_{\text{DM,eff}}$, $c_{\text{sDE,eff}}^2$ and Best-fit χ^2 for Phantom (non)Interacting Models under Consideration using *Planck*, *Planck+R16*, and *Planck+BSH*

Data	Model	Ω_{0m}	H_0	σ_8	w_0	w_a	$w_{\text{DM,eff}}$	$c_{\text{sDE,eff}}^2$	χ_{bf}^2	$\chi_{\Lambda\text{CDM}}^2 - \chi_{\text{bf}}^2$
<i>Planck</i>	ΛCDM	$0.30^{+0.02}_{-0.02}$	$68.1^{+1.2}_{-1.2}$	$0.85^{+0.03}_{-0.02}$	-1	0	0	1	781.07	0
	CPLCDM	$0.19^{+0.02}_{-0.04}$	$88.4^{+11.6}_{-3.7}$	$1.02^{+0.08}_{-0.06}$	$-1.5^{+0.3}_{-0.3}$	$-0.13^{+0.27}_{-0.03}$	0	1	779.83	-1.24
	+ $w_{\text{DM,eff}}$	$0.62^{+0.32}_{-0.59}$	$66.7^{+32.0}_{-11.1}$	$0.80^{+0.27}_{-0.13}$	$-2.0^{+1.0}_{-1.0}$	$-0.45^{+0.48}_{-1.50}$	$-0.0075^{+0.005}_{-0.004}$	1	778.26	-2.81
	+ $c_{\text{sDE,eff}}^2$	$0.68^{+0.32}_{-0.66}$	$64.9^{+31.7}_{-13.5}$	$0.79^{+0.28}_{-0.14}$	$-2.0^{+1.0}_{-1.0}$	$-0.42^{+0.49}_{-1.58}$	$-0.0078^{+0.005}_{-0.004}$	$1.03^{+0.84}_{-0.45}$	778.88	-2.19
<i>Planck</i> +R16	ΛCDM	$0.29^{+0.01}_{-0.01}$	$69.7^{+1.0}_{-1.0}$	$0.86^{+0.02}_{-0.02}$	-1	0	0	1	786.66	0
	CPLCDM	$0.26^{+0.01}_{-0.01}$	$74.0^{+1.7}_{-1.7}$	$0.90^{+0.02}_{-0.03}$	$-1.1^{+0.1}_{-0.1}$	$-0.27^{+0.46}_{-0.26}$	0	1	782.02	-4.64
	+ $w_{\text{DM,eff}}$	$0.29^{+0.02}_{-0.02}$	$74.5^{+2.1}_{-2.1}$	$0.88^{+0.03}_{-0.03}$	$-2.0^{+1.0}_{-1.0}$	$-0.96^{+1.10}_{-1.50}$	$-0.005^{+0.001}_{-0.003}$	1	777.65	-9.01
	+ $c_{\text{sDE,eff}}^2$	$0.29^{+0.02}_{-0.02}$	$74.5^{+2.1}_{-2.2}$	$0.89^{+0.02}_{-0.02}$	$-2.0^{+1.0}_{-1.0}$	$-0.94^{+1.05}_{-1.65}$	$-0.005^{+0.001}_{-0.002}$	$1.03^{+0.96}_{-0.34}$	780.19	-6.47
<i>Planck</i> +BSH	ΛCDM	$0.30^{+0.01}_{-0.01}$	$68.5^{+0.6}_{-0.6}$	$0.86^{+0.02}_{-0.02}$	-1	0	0	1	1490.66	0
	CPLCDM	$0.29^{+0.01}_{-0.01}$	$69.8^{+1.0}_{-1.0}$	$0.87^{+0.02}_{-0.02}$	$-1.05^{+0.05}_{-0.01}$	$-0.15^{+0.21}_{-0.10}$	0	1	1490.29	-0.37
	+ $w_{\text{DM,eff}}$	$0.30^{+0.01}_{-0.01}$	$69.7^{+1.0}_{-1.0}$	$0.86^{+0.02}_{-0.02}$	$-1.06^{+0.06}_{-0.01}$	$-0.33^{+0.39}_{-0.19}$	$-0.0012^{+0.001}_{-0.001}$	1	1488.14	-2.52
	+ $c_{\text{sDE,eff}}^2$	$0.30^{+0.01}_{-0.01}$	$69.7^{+1.0}_{-1.0}$	$0.86^{+0.02}_{-0.02}$	$-1.06^{+0.06}_{-0.01}$	$-0.34^{+0.40}_{-0.18}$	$-0.0012^{+0.001}_{-0.001}$	$1.02^{+0.98}_{-1.02}$	1488.83	-1.83

Note. Corresponding values for ΛCDM and CPLCDM are given for comparison.

higher values of Ω_{0m} . The *Planck* results therefore have the potential to be commensurate with the cluster results, since $\Omega_{0m} = 0.3$, $\sigma_8 = 0.75$ falls well within the 1σ levels (gray contours of middle panel). However, both BAO and H_0 measurements appear to push σ_8 to higher values, mainly because σ_8 has a positive correlation with H_0 , i.e., the higher H_0 , the higher the value of σ_8 . Thus by increasing the value of H_0 to fit BSH, we reduce consistency with cluster results for σ_8 , since lower H_0 and therefore lower σ_8 are disfavored when these data sets are added to *Planck* (red and blue contours of left and middle panels).

The effective equation of state of dark energy is constrained only with the addition of BAO and SNe data: while $w_0 \simeq -1.2$ at 2σ , the rate of change w_a is allowed a fairly large range, going down to $w_a \gtrsim -1.6$.

We are now in a position to make use of these results to compare among different types of models under consideration, some of which have a smaller number of free parameters (namely ΛCDM or non-interacting $w_2\text{CDM}$ with phantom-like behavior using the CPL ansatz for w_{DE} again). We can readily do so by comparing the best-fit, 1σ values for the different parameters, as well as the best-fit χ^2 in Table 1. We see that for *Planck* data only, χ^2 for CPLCDM is slightly better than that

for ΛCDM , although not at a significance where it could be comprehensively claimed that phantom variable dark energy models are favored over ΛCDM . Introducing $w_{\text{DM,eff}}$, which is equivalent to introducing a coupling between DM and DE (or introducing warm dark matter models), does improve χ^2 over ΛCDM slightly more in the phantom case. The addition of the parameter $c_{\text{sDE,eff}}^2$, on the contrary, degrades χ^2 very slightly, possibly because the parameter space now has too many degeneracies, thus reducing the constraining abilities of the data. We also see that for just *Planck* data, CPLCDM may allow much higher values of H_0 than ΛCDM does, but for lower values of Ω_{0m} . In fact, the value chosen for H_0 is so high that it is now incommensurate with R16, but from the higher end, with a lower Ω_{0m} to boot. Thus we cannot achieve consistency between *Planck* and R16 by simply allowing dynamical DE in the phantom regime. When BAO and SNe are added, Ω_{0m} increases, reducing the value of H_0 again to ΛCDM levels, so putting all the data together results in constraints very similar to that for ΛCDM , albeit with a slightly better χ^2 . The addition of $w_{\text{DM,eff}}$ opens up the H_0 parameter space, and a much larger range of values is allowed for both H_0 and Ω_{0m} , for even a slightly non-zero value of $w_{\text{DM,eff}}$. Thus consistency with R16 is achieved with $\Omega_{0m} \simeq 0.3$. Once again, however,

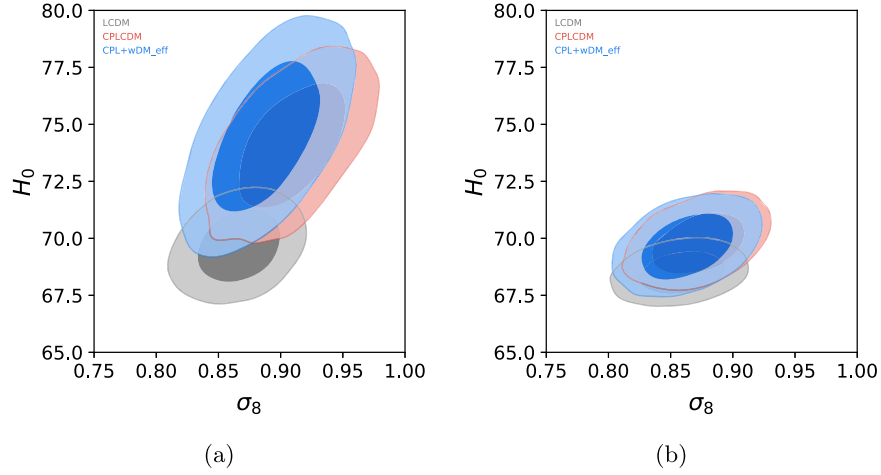


Figure 3. 1σ and 2σ confidence levels in the $H_0 - \sigma_8$ parameter spaces using *Planck*+**R16** (left panel) and *Planck*+BSH (right panel) for (i) Λ CDM models (gray), (ii) CPLCDM models (red), and (iii) (non)phantom interacting models (blue) under consideration.

the addition of BAO and SNe constrains $w_{\text{DM,eff}} \simeq 0$, bringing the value of H_0 down slightly, although it is still higher than that for Λ CDM. For σ_8 , we find that the *Planck* data alone do allow for a lower σ_8 for reasonable values of Ω_{0m} . However, the addition of **R16**, or of BSH, increases σ_8 in response to the corresponding increase in H_0 . The σ_8 parameter may take on lower values for just *Planck* data, but it still appears to favor higher values when all data are taken together, so the tension with cluster data remains unresolved.

So, in a nutshell, the results for the phantom case can be summarized as below.

1. H_0 tension:

- (a) **R16**: gives high H_0 .
- (b) CMB: Λ CDM prefers low H_0 ; non-interacting CPLCDM has too high H_0 and too low Ω_{0m} . In comparison, in this class of interacting CPLCDM or warm dark matter models, Ω_{0m} is fairly unconstrained, hence although a positive correlation between H_0 and Ω_{0m} remains, it is possible to obtain high H_0 to **R16** levels for a large range of Ω_{0m} , which is a distinct improvement over both Λ CDM and CPLCDM.
- (c) BAO: Λ CDM and non-interacting CPLCDM both prefer low H_0 (or possibly high Ω_{0m}). Interacting CPLCDM too appears to prefer slightly low H_0 , but it is more in line with the **R16** value, therefore the tension between H_0 and CMB can be partially resolved even after the addition of BAO data.
- (d) JLA: Since this data set prefers non-phantom dark energy, and *Planck* prefers negative $w_{\text{DM,eff}}$, addition of this data set can only serve to increase Ω_{0m} and therefore decrease H_0 , thus exacerbating the tension with the high value of H_0 obtained by **R16**.
- (e) Therefore for the CPLCDM case, tension between **R16** and *Planck* is resolved for reasonable values of Ω_{0m} , which is not possible for both Λ CDM and CPLCDM. However, the tension between BAO and H_0 is only partially resolved, and addition of SNe data makes the tension with H_0 reappear.

2. σ_8 tension:

- (a) Clusters prefer low σ_8 .
- (b) CMB: Λ CDM prefers low H_0 , but not low enough to allow cluster σ_8 . For non-interacting CPLCDM, addition of CPL causes opening-up of parameter

space with higher H_0 and σ_8 . So one cannot get low σ_8 , and the tension becomes worse. However, for this class of interacting CPLCDM or warm dark matter models, addition of $w_{\text{DM,eff}}$ causes opening-up of parameter space, for both higher and lower H_0 and σ_8 , therefore tension with clusters is resolved if we allow lower H_0 .

- (c) CMB+**R16**: For Λ CDM and CPLCDM, there is no improvement over the CMB result. For interacting CPLCDM as well, higher σ_8 is preferred because **R16** prefers higher values of H_0 due to positive correlation between σ_8 and H_0 .
- (d) CMB+BSH: For Λ CDM and CPLCDM we see no improvement over the CMB result; higher H_0 means higher σ_8 . However, for interacting CPLCDM, slightly lower H_0 is preferred (due to the presence of BAO and SNe data), therefore slightly lower σ_8 is also allowed, although not enough to resolve tension with clusters. This, however, comes at the cost of inconsistency with the **R16** measurements of H_0 .

It transpires from the above discussion that there appears to be a positive correlation between H_0 and σ_8 , no matter whether we choose Λ CDM, non-interacting w_c CDM, warm dark matter or a wide class of interacting DMDE as the cosmological model. In order to express this positive correlation in a more concrete language, we have plotted the 1σ and 2σ confidence levels in the $H_0 - \sigma_8$ parameter space in Figure 3. To compare among different data sets, we show the confidence levels for *Planck*+**R16** in the left panel and *Planck*+BSH in the right panel, for (i) Λ CDM models (gray contours), (ii) phantom CPLCDM models (red contours), and (iii) phantom interacting DMDE models (blue contours). We see that as we free up more parameters, the correlation becomes more significant in the case of *Planck*+**R16** although we confine the parameter space to comparatively higher values of H_0 (due to **R16**). For *Planck*+BSH, the correlation is relatively less apparent due to the use of BAO and SNe data, which confine the results to the low H_0 space. Thus, the positive correlation appears to be generic to CMB data, and this persists even after adding the low-redshift data sets; hence a higher H_0 is simply not consistent with a low σ_8 , and both the tensions cannot be simultaneously resolved, at least for a fairly general class of cosmological models using present data sets.

Thus from this section we find, first, that phantom DE models are very slightly favored (or at least not disfavored) over Λ CDM, and allowing even a very small interaction between DM and DE does provide an even better fit to the CMB data. Varying the sound speed of dark energy does not improve the fit. Second, we note that the tension between direct measurement of H_0 and *Planck* measurement of H_0 can be eased by introduction of a small, negative $w_{\text{DM,eff}}$. This implies that a class of interacting dark energy models with energy transfer from dark energy to dark matter, with a more phantom dark energy EoS and a slower rate of redshift of dark matter, can resolve this tension. When all the data are put together, a slightly negative $w_{\text{DM,eff}}$ and slightly phantom w_0 (and negative w_a , implying that dark energy was even more phantom-like in the past) are still favored over Λ CDM. Therefore, a major success of our analysis making use of an effective phantom EoS is that it gives rise to a consistent H_0 for CMB+R16 with a considerably good value of Ω_{DM} at least for a class of interacting DMDE models. Thus, this class of models with an effective phantom EoS gets a slight edge over the others as far as present data are concerned. Lastly, the bottom line for the σ_8 tension is that non-interacting $w_{\text{z}}\text{CDM}$ cannot resolve tension between clusters and *Planck* CDM. This type of interacting CPLCDM can resolve tension if lower H_0 is allowed. If, however, H_0 is high, we cannot get low σ_8 from CMB; therefore tension of CMB with H_0 and σ_8 can be resolved separately, but not together. However, since the effective EoS for dark matter $w_{\text{DM,eff}}$ prefers a slightly negative value, warm dark matter models are not that favored compared to this class of interacting models.

We remind the curious reader that the EoS for dark matter is the effective EoS even though the actual EoS may indicate CDM. An effective negative EoS for dark matter, as obtained in Table 1, may be looked upon as follows. A class of interacting DMDE models where energy transfer happens from dark energy to dark matter are slightly preferred. In this regard, it is interesting to point out that there exists a well studied model where a simple Yukawa-type interaction between a dark matter fermion and a dark energy scalar $\exp\left(\frac{\beta\phi}{M_{\text{p}}}\right)\bar{\psi}_{\text{DM}}\psi_{\text{DM}}$ with a runaway scalar potential automatically transfers energy to dark matter from dark energy with $\beta > 0$ (Damour & Polyakov 1994; Amendola 2000; Das et al. 2006). This type of model with positive β can have its origin naturally in string theory. Due to this energy intake over Hubble time, dark matter redshifts more slowly than $1/a^3$ and as a result acquires an effective negative equation of state.

4.2. Non-phantom EoS

We now look at the same data sets in the non-phantom, i.e., $w_{\text{DE,eff}} \geq -1$, space for the same class of models, namely Λ CDM, non-interacting CPLCDM, warm dark matter as well as a class of interacting DMDE models. In this case too, $c_{\text{s,DE,eff}}^2$ has minimal effect on the results. Figure 4 shows the likelihoods for the remaining six parameters. Unlike in the previous case, *Planck* data alone (black) show a preference for much lower H_0 and much higher Ω_{DM} . The parameter $w_{\text{DM,eff}}$ is still negative, but the likelihoods for Ω_{DM} , H_0 , σ_8 , $w_{\text{DM,eff}}$ in the case of *Planck* all appear to be inconsistent with those for *Planck*+R16 (red) and *Planck*+BSH (blue). This shows that for the non-phantom scenario, *Planck* CMB results are at odds with those from other data. Figure 5 shows the 1σ and 2σ

confidence levels for $H_0 - w_{\text{DM,eff}}$, $\Omega_{\text{DM}} - \sigma_8$ and $w_0 - w_a$. Whereas in the phantom case the extra parameter was liberating both high and low values of H_0 , here we see that the $H_0 - w_{\text{DM,eff}}$ confidence levels are inconsistent with those from other data at nearly 2σ . Low values of matter density are strongly disfavored, as well as high values of σ_8 , once again making *Planck* by itself inconsistent with other data sets. The equation of state of dark energy appears to be more constrained than in the phantom case when all data are considered, leaving very little flexibility. Thus here the tension in H_0 is not resolved because lower values of H_0 are so strongly favored by *Planck*; neither is the σ_8 tension eased.

We compare these results against different models under consideration, namely Λ CDM, non-interacting CPLCDM, a class of interacting CPLCDM, and warm dark matter in Table 2. In the non-phantom scenario, for all data sets, it appears that Λ CDM has better χ^2 than CPLCDM as well as interacting models. The addition of $w_{\text{DM,eff}}$ improves χ^2 slightly from the CPLCDM scenario, but it is still greater than that of Λ CDM. Therefore we may conclude that the cosmological constant is favored over non-phantom dark energy models, even when we include an interaction in the dark sector. As expected, even with the added parameters, the best-fit values for the standard parameters Ω_{DM} , H_0 , σ_8 are pretty close to the Λ CDM values; even the dark energy parameters are close to $w_0 = -1$ and $w_a = 0$. When all data are considered, $w_{\text{DM,eff}}$ has a slightly positive value, but as noted before, this is not statistically favored over Λ CDM. We note here that the JLA SNe data are probably the only data set that favors non-phantom w_{DE} over phantom w_{DE} , but as the other data sets strongly disfavor non-phantom, the effect of JLA is not felt in these results. Here also $w_{\text{DM,eff}}$ is still slightly negative, disfavoring warm dark matter models, at least from present data sets.

As in the case of phantom EoS, here also a positive correlation between H_0 and σ_8 is apparent. This has been depicted in Figure 6. To compare among different data sets, we have plotted 1σ and 2σ confidence levels in the $H_0 - \sigma_8$ parameter spaces using *Planck*+R16 in the left panel and *Planck*+BSH in the right panel for (i) Λ CDM (gray), (ii) CPLCDM (red), and (iii) non-phantom interacting DMDE (blue) models. These plots reveal a positive correlation between these two parameters for the non-phantom case as well.

In totality, therefore, we may conclude from the above analysis that phantom dark energy is preferred over non-phantom by most of the present data sets except JLA SNe. In the phantom $w_{\text{DE,eff}} \leq -1$ regime, the addition of a very small interaction term ($w_{\text{DM,eff}} \sim -0.001$, implying transfer of energy from dark energy to dark matter) improves the fit over Λ CDM, and also eases the tension between *Planck* and direct H_0 measurements, allowing for a very negative $w_{\text{DE,eff}}$. Addition of BAO and SNe causes the equation of state of dark energy to move closer to Λ CDM, thus reintroducing a slight tension in H_0 . This is due to inconsistencies within the BSH data: BAO prefers lower H_0 than R16, SNe does not constrain H_0 but prefers non-phantom DE, and when restricted to phantom and to $w_{\text{DM,eff}} < 0$ from CMB, it increases Ω_{DM} , thereby lowering H_0 as compared to both BAO and R16. σ_8 from *Planck* alone is lower for phantom models, whereas that for *Planck*+BSH remains at the higher end, thus the tension with cluster counts remains for interacting dark energy models when all data are considered. Overall, we find that the addition

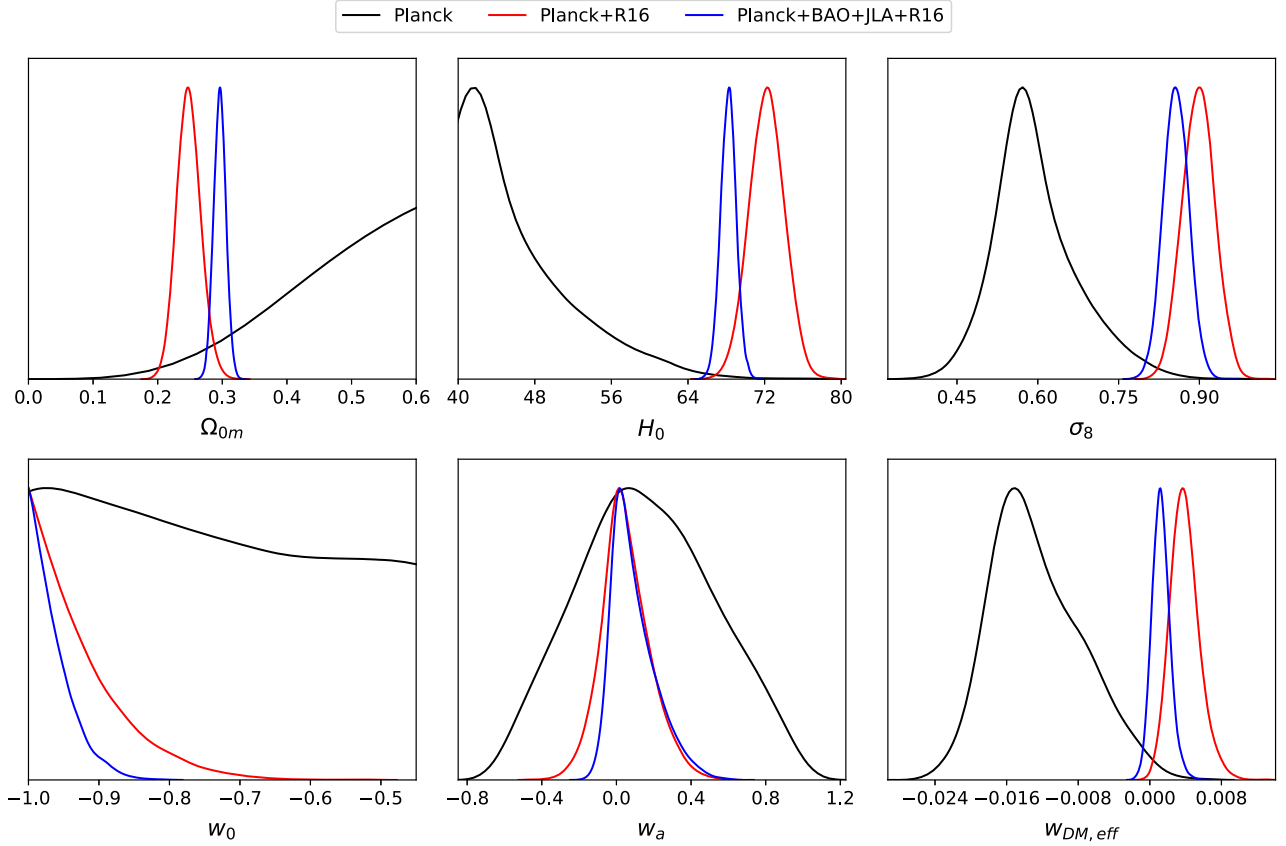


Figure 4. Likelihoods in Ω_{0m} , H_0 , σ_8 , w_0 , w_a , $w_{DM,eff}$ for cosmological reconstruction using *Planck* (black lines), *Planck+R16* (red lines), and *Planck+BSH* (blue lines) for non-phantom (non)interacting models under consideration.

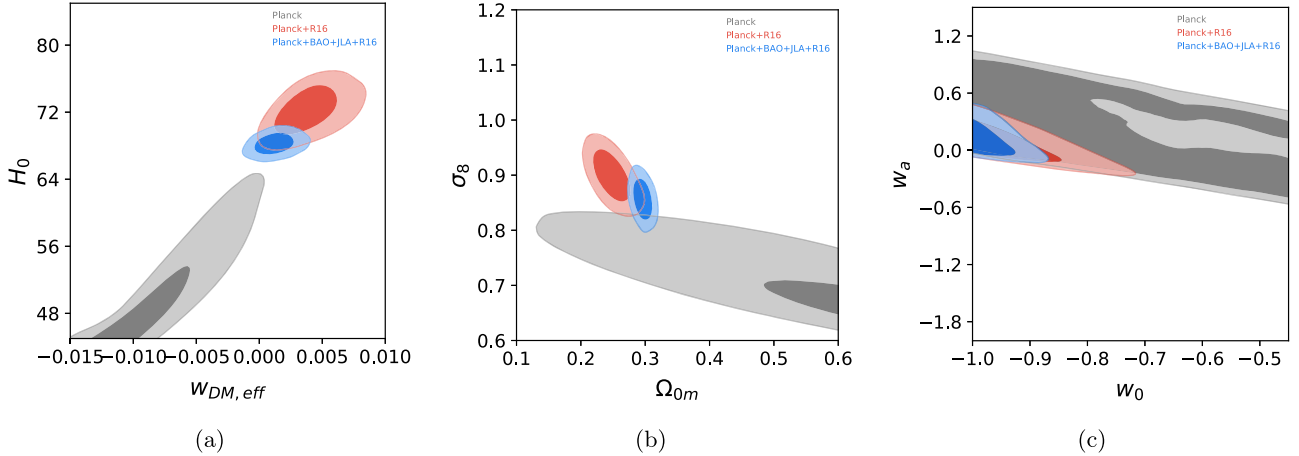


Figure 5. 1σ and 2σ confidence levels in the $H_0 - w_{DM,eff}$ (left panel), $\Omega_{0m} - \sigma_8$ (middle panel), and $w_0 - w_a$ (right panel) parameter spaces using *Planck* (gray), *Planck+R16* (red), and *Planck+BSH* (blue) for non-phantom (non)interacting DMDE models under consideration.

of a small negative $w_{DM,eff}$ for phantom DMDE models ($w_{DE,eff} \leq -1$) improves the fit with the data, and eases the tension between **R16** and *Planck*. The positive correlation between H_0 and σ_8 appears to be generic to the CMB data, for both phantom and non-phantom DE EoSs. Hence both the tensions cannot be simultaneously resolved, at least for a wide class of cosmological models using present data sets.

5. Conclusions

In this article, we have attempted to investigate the well-known inconsistencies between different cosmological data

sets in a model-independent framework that takes into account different classes of cosmological models (Λ CDM, non-interacting w_z CDM, modified gravity, warm dark matter, as well as a class of interacting DMDE models). As is well known, there is a tension among CMB, **R16**, and BAO data on preferred values of H_0 . Also, CMB data are at odds with cluster data as far as the value of σ_8 is concerned. In this article, we tried to check whether one can alleviate these tensions simultaneously, and if so, whether the choice of cosmological models plays a significant role. Our major findings are summarized below.

Table 2Best-fit and 1σ Values for Ω_{0m} , H_0 , σ_8 , w_0 , w_a , $w_{DM,eff}$, $c_{sDE,eff}^2$ and Best-fit χ^2 for Non-phantom (non)Interacting Models under Consideration using *Planck*, *Planck*+**R16**, and *Planck*+BSH

Data	Model	Ω_{0m}	H_0	σ_8	$w_{0,eff}$	$w_{a,eff}$	$w_{DM,eff}$	$c_{sDE,eff}^2$	χ_{bf}^2	$\chi_{\Lambda CDM}^2 - \chi_{bf}^2$
<i>Planck</i>	Λ CDM	$0.30^{+0.02}_{-0.02}$	$68.1^{+1.2}_{-1.2}$	$0.85^{+0.03}_{-0.02}$	-1	0	0	1	781.07	0
	CPLCDM	$0.37^{+0.03}_{-0.05}$	$62.5^{+4.0}_{-2.7}$	$0.80^{+0.04}_{-0.03}$	$-0.82^{+0.14}_{-0.18}$	$0.03^{+0.22}_{-0.22}$	0	1	782.75	1.68
	+ $w_{DM,eff}$	$1.06^{+0.31}_{-0.47}$	$44.0^{+4.3}_{-7.5}$	$0.60^{+0.05}_{-0.08}$	$-0.68^{+0.35}_{-0.32}$	$0.16^{+0.36}_{-0.40}$	$-0.012^{+0.004}_{-0.006}$	1	782.63	1.56
	+ $c_{sDE,eff}^2$	$1.03^{+0.33}_{-0.43}$	$44.5^{+3.7}_{-8.0}$	$0.60^{+0.04}_{-0.09}$	$-0.68^{+0.05}_{-0.35}$	$0.16^{+0.36}_{-0.40}$	$-0.012^{+0.003}_{-0.006}$	$0.98^{+1.02}_{-0.98}$	780.58	-0.49
<i>Planck</i> + R16	Λ CDM	$0.29^{+0.01}_{-0.01}$	$69.7^{+1.0}_{-1.0}$	$0.86^{+0.02}_{-0.02}$	-1	0	0	1	786.66	0
	CPLCDM	$0.29^{+0.01}_{-0.01}$	$68.6^{+1.3}_{-1.1}$	$0.85^{+0.02}_{-0.02}$	$-0.97^{+0.01}_{-0.03}$	$0.03^{+0.04}_{-0.06}$	0	1	788.97	2.31
	+ $w_{DM,eff}$	$0.25^{+0.02}_{-0.02}$	$72.2^{+1.8}_{-1.8}$	$0.89^{+0.03}_{-0.03}$	$-0.92^{+0.01}_{-0.08}$	$0.05^{+0.48}_{-0.13}$	$0.004^{+0.001}_{-0.001}$	1	785.81	-0.85
	+ $c_{sDE,eff}^2$	$0.25^{+0.02}_{-0.02}$	$72.2^{+1.8}_{-1.8}$	$0.89^{+0.03}_{-0.03}$	$-0.92^{+0.01}_{-0.08}$	$0.05^{+0.10}_{-0.59}$	$0.004^{+0.001}_{-0.002}$	$1.94^{+0.06}_{-1.94}$	785.73	-0.93
<i>Planck</i> +BSH	Λ CDM	$0.30^{+0.01}_{-0.01}$	$68.5^{+0.6}_{-0.6}$	$0.86^{+0.02}_{-0.02}$	-1	0	0	1	1490.66	0
	CPLCDM	$0.30^{+0.01}_{-0.01}$	$67.8^{+0.7}_{-0.7}$	$0.85^{+0.02}_{-0.02}$	$-0.97^{+0.01}_{-0.03}$	$0.04^{+0.04}_{-0.08}$	0	1	1493.36	2.70
	+ $w_{DM,eff}$	$0.30^{+0.01}_{-0.01}$	$68.2^{+0.8}_{-0.8}$	$0.85^{+0.02}_{-0.02}$	$-0.96^{+0.01}_{-0.04}$	$0.10^{+0.07}_{-0.14}$	$0.0012^{+0.001}_{-0.001}$	1	1491.01	0.35
	+ $c_{sDE,eff}^2$	$0.30^{+0.01}_{-0.01}$	$68.2^{+0.8}_{-0.8}$	$0.86^{+0.02}_{-0.02}$	$-0.96^{+0.01}_{-0.04}$	$0.09^{+0.06}_{-0.14}$	$0.0012^{+0.001}_{-0.001}$	$0.98^{+1.02}_{-0.98}$	1491.59	0.93

Note. Corresponding values for Λ CDM and CPLCDM are given for comparison.

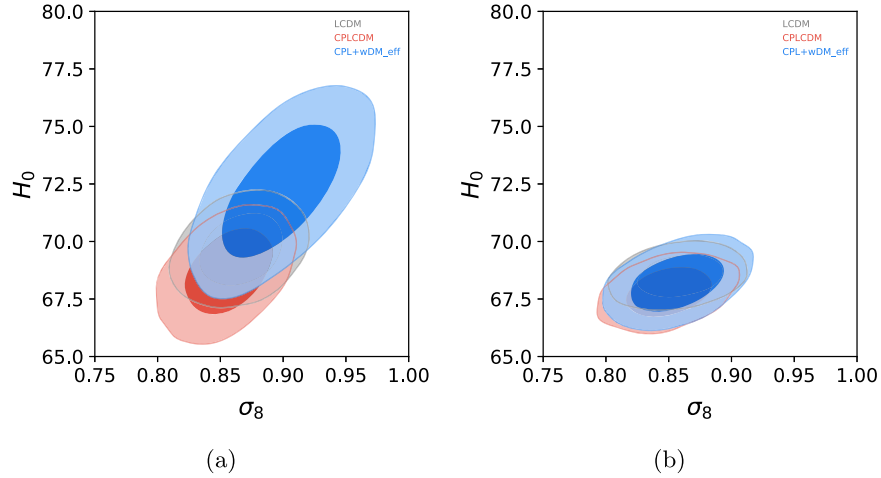


Figure 6. 1σ and 2σ confidence levels in the H_0 - σ_8 parameter spaces using *Planck*+**R16** (left panel) and *Planck*+BSH (right panel) for (i) Λ CDM (gray), CPLCDM (red), and non-phantom (non)interacting (blue) models under consideration.

1. A strong positive correlation between σ_8 and H_0 is more or less generic for the data, irrespective of the choice of cosmological models (Λ CDM/ w_z CDM/warm dark matter/a wide class of interacting dark sectors). The positive correlation appears to be inbuilt in the CMB data themselves, and is true for both phantom and non-phantom EoSs for dark energy. If one gets a higher value, the other also shoots up, and vice versa. Since **R16** prefers high H_0 , and cluster data prefer low σ_8 as compared to CMB, both the tensions cannot be simultaneously resolved, at least using present data sets.
2. Present data slightly prefer a phantom equation of state for dark energy and a slightly negative value for the effective equation of state for dark matter (which in turn signifies an energy flow from dark energy to dark matter, and at the same time disfavors warm dark matter models), and for this scenario the use of more parameters opens up *Planck* parameter space wide so that high H_0 is allowed by *Planck*, which is otherwise not achievable in the minimal six-parameter Λ CDM or CPLCDM cosmology. This comparatively higher value of H_0 is consistent with *Planck*+**R16** data for direct measurement of H_0 but is in

- tension with BAO and SNe data (and hence with BSH data) since these prefer a lower value for H_0 .
3. Along with a high H_0 we also achieve a consistent value for $\Omega_{0m} \sim 0.3$ for interacting dark sectors. So, at least, one can resolve H_0 versus *Planck* tension with a reasonable value for Ω_{0m} if one allows interaction, which could not be achieved either in the Λ CDM model or in non-interacting w_z CDM models. This is a clear advantage of a wide class of interacting DMDE models over the others. These models with an effective phantom EoS get a slight edge over the others as far as present data are concerned.
4. Freeing up some parameters (and thereby opening up the interacting dark sector) allows us to have a comparatively lower value of σ_8 (compared to Λ CDM or w_z CDM) from *Planck* alone. However, when *Planck* data are taken together with BSH, it rises again and becomes inconsistent with cluster counts. A value for σ_8 that is consistent with cluster counts is achievable for *Planck* alone, or with SNe data, but this would lead to an H_0 in tension with both galaxy BAO and **R16** data.

5. Thus it is possible to alleviate the tension between the high-redshift CMB data and individual low-redshift data sets by changing the expansion history of the universe to include at least a class of interacting DMDE models. However, the low-redshift data have inconsistencies within themselves so that it is not possible to match all the low-redshift data sets to CMB simultaneously. Here we have explored these underlying tensions within low-redshift data sets, which have not been explored earlier. For example, CMB data can reach the high H_0 from R16, but this leads to a high σ_8 as well, which is problematic from cluster counts. CMB and SNe data can together achieve low σ_8 to match cluster counts, but only for an H_0 much lower than that for R16 or BAO. BAO chooses an H_0 that is typically lower than that from R16, but not low enough to then be consistent with the σ_8 from cluster counts. SNe data prefer a non-phantom EoS for DE and are therefore in tension with most other data sets. So, the usual practice of using BSH data, and thereby clubbing R16, BAO, and JLA together, with all their internal inconsistencies, may not be a wise method for the estimation of cosmological parameters.
6. For the non-phantom (quintessence) case, the results are not too encouraging, which resonates with earlier findings that a phantom EOS for dark energy is slightly favored as far as present data are concerned. However, for the non-phantom case as well, there are direct indications of a strong positive correlation between σ_8 and H_0 . This is in tune with our conclusion that one cannot simultaneously resolve both the tensions, no matter whether one considers Λ CDM, non-interacting w_z CDM, or a wide class of phantom or non-phantom interacting dark sectors.

In conclusion, we reiterate: that phantom dark energy with an energy flow from dark energy to dark matter is slightly preferred over other classes of models for the present data set; that the low-redshift BSH data have inconsistencies within themselves and with CMB, and using all the data in conjunction does not necessarily give a true picture of the universe; and lastly that it is not possible to achieve low σ_8 and high H_0 simultaneously for a wide class of DE models using present data sets.

We gratefully acknowledge use of the publicly available code CosmoMC. We also thank computational facilities of ISI Kolkata and IIA Bangalore, and especially Mr. Anish Parwage for setting up the computing facilities at IIA for CosmoMC runs. A.B. thanks DST, India for financial support through INSPIRE fellowship DST-INSPIRE/IF150497. U.A. was purportedly supported through the Young Scientist Grant YSS/2014/000096 of DST, India.

ORCID iDs

Kanhaiya Lal Pandey  <https://orcid.org/0000-0003-3536-1730>

References

Ade, P. A. R., Aghanim, N., Arnaud, M., et al. 2016, *A&A*, 594, A24
 Aghamousa, A., Hamann, J., & Shafieloo, A. 2017, *JCAP*, 09, 031
 Alam, S., Ata, M., Bailey, S., et al. 2017, *MNRAS*, 470, 2617

Alam, U. 2010, *ApJ*, 714, 1460
 Alam, U., Bag, S., & Sahni, V. 2017, *PhRvD*, 9, 023524
 Alam, U., & Lasue, J. 2017, *JCAP*, 1706, 034
 Amendola, L. 1999, *PhRvD*, 60, 043501
 Amendola, L. 2000, *PhRvD*, 62, 043511
 Amendola, L. 2004, *PhRvD*, 69, 103524
 Aubourg, É., Bailey, S., Bautista, J. E., et al. 2015, *PhRvD*, 92, 123516
 Bahamonde, S., Böhmer, C. G., Carloni, S., et al. 2018, *PhR*, 775, 1
 Bean, R., Flanagan, E. E., Laszlo, I., & Trodden, M. 2008, *PhRvD*, 78, 123514
 Betoule, M., Kessler, R., Guy, J., et al. 2014, *A&A*, 568, A22
 Beyer, J., Nurmi, S., & Wetterich, C. 2011, *PhRvD*, 84, 023010
 Bilyard, A. P., & Coley, A. A. 2000, *PhRvD*, 61, 083503
 Boehmer, C. G., Caldera-Cabral, G., Lazkoz, R., & Maartens, R. 2008, *PhRvD*, 78, 023505
 Bohringer, H., Chon, G., & Collins, C. A. 2014, *A&A*, 570, A31
 Bonvin, V., Courbin, F., Suyu, S. H., et al. 2017, *MNRAS*, 465, 4914
 Busti, V. C., & Clarkson, C. 2016, *JCAP*, 05, 008
 Chen, Y., Kumar, S., & Ratra, B. 2017, *ApJ*, 835, 86
 Chevallier, M., & Polarski, D. 2001, *IJMPD*, 10, 213
 Chimento, L. P., Jakubi, A. S., Pavon, D., & Zimdahl, W. 2003, *PhRvD*, 67, 083513
 Clifton, T., Ferreira, P. G., Padilla, A., & Skordis, C. 2012, *PhR*, 513, 1
 Comelli, D., Pietroni, M., & Riotto, A. 2003, *PhLB*, 571, 115
 Copeland, E. J., Sami, M., & Tsujikawa, S. 2006, *IJMPD*, 15, 1753
 Damour, T., & Polyakov, A. M. 1994, *NuPhB*, 423, 532
 Das, S., Corasaniti, P. S., & Khoury, J. 2006, *PhRvD*, 73, 083509
 Delubac, T., Bautista, J. E., Busca, N. G., et al. 2014, *A&A*, 574, A59
 Di Valentino, E., Melchiorri, A., Linder, E. V., & Silk, J. 2017, *PhRvD*, 96, 023523
 Di Valentino, E., Melchiorri, A., & Mena, O. 2017, *PhRvD*, 96, 043503
 Durrer, R., & Maartens, R. 2010, in *Dark Energy: Observational & Theoretical Approaches*, ed. P. Ruiz-Lapuente (Cambridge: Cambridge Univ. Press), 48
 Efstathiou, G. 2014, *MNRAS*, 440, 1138
 Fang, W., Hu, W., & Lewis, A. 2008, *PhRvD*, 78, 087303
 Farrar, G. R., & Peebles, P. J. E. 2004, *ApJ*, 604, 1
 Frieman, J. A., Turner, M. S., & Huterer, D. 2008, *ARA&A*, 46, 385
 Gómez-Valent, A., & Amendola, L. 2018, *JCAP*, 1804, 051
 Holden, D. J., & Wands, D. 2000, *PhRvD*, 61, 043506
 Holsclaw, T., Alam, U., Sansó, B., et al. 2010, *PhRvL*, 105, 241302
 Hwang, J. C., & Noh, H. 2002, *CQGrA*, 19, 527
 Karwal, T., & Kamionkowski, M. 2016, *PhRvD*, 94, 103523
 Kumar, S., & Nunes, R. C. 2017, *EPJC*, 77, 734
 Lazkoz, R., Salzano, V., & Sendra, I. 2012, *EPJC*, 72, 2130
 Linder, E. V. 2003, *PhRvL*, 90, 091301
 Lopez Honorez, L., Mena, O., & Panotopoulos, G. 2010, *PhRvD*, 82, 123525
 Mantz, A. B., Linden, A. V. D., Allen, S. W., et al. 2015, *MNRAS*, 446, 2205
 Mishra, S. S., & Sahni, V. 2018, arXiv:1803.09767
 Moresco, M., & Marulli, F. 2017, *MNRAS*, 471, L82
 Mortonson, M. J., Weinberg, D. H., & White, M. 2014, arXiv:1401.0046
 Nojiri, S., & Odintsov, S. D. 2011, *PhR*, 505, 59
 Padmanabhan, T. 2003, *PhR*, 380, 235
 Pavan, A., Ferreira, E. G., Micheletti, S., de Souza, J., & Abdalla, E. 2012, *PhRvD*, 86, 103521
 Peebles, P. J. E., & Ratra, B. 2003, *RvMP*, 75, 559
 Pettorino, V., Amendola, L., Baccigalupi, C., & Quercellini, C. 2012, *PhRvD*, 86, 103507
 Pourtsidou, A., Skordis, C., & Copeland, E. 2013, *PhRvD*, 88, 083505
 Riess, A. G., Macri, L., Casertano, S., et al. 2011, *ApJ*, 730, 119
 Riess, A. G., Macri, L. M., Hoffmann, S. L., et al. 2016, *ApJ*, 826, 56
 Sahni, V. 2004, *Lecture Notes in Physics*, Vol. 653 (Berlin: Springer), 141
 Sahni, V., & Starobinsky, A. A. 2000, *IJMPD*, 9, 373
 Shafieloo, A., Kim, A. G., & Linder, E. V. 2013, *PhRvD*, 87, 023520
 Tammann, G. A., & Reindl, B. 2013, *A&A*, 549, A136
 Tarrant, E. R., van de Bruck, C., Copeland, E. J., & Green, A. M. 2012, *PhRvD*, 85, 023503
 Tsujikawa, S. 2010, *Dark Matter and Dark Energy: a Challenge for the 21st Century*, arXiv:1004.1493
 Valiviita, J., Majerotto, E., & Maartens, R. 2008, *JCAP*, 0807, 020
 Valiviita, J., & Palmgren, E. 2015, *JCAP*, 1507, 015
 Yu, H., Ratra, B., & Wang, F.-Y. 2018, *ApJ*, 856, 3
 Zhai, Z., Blanton, M., Slosar, A., & Tinker, J. 2017, *ApJ*, 850, 183
 Zhao, G.-B., Crittenden, R. G., Pogosian, L., & Zhang, X. 2012, *PhRvL*, 109, 171301
 Zimdahl, W., & Pavon, D. 2001, *PhLB*, 521, 133